ISSN: 2447-3359

REVISTA DE GEOCIÊNCIAS DO NORDESTE

Northeast Geosciences Journal

v. 11, nº 1 (2025)

https://doi.org/10.21680/2447-3359.2025v11n1ID39238

Analysis of the behavior of PPP and ionospheric TEC in the post-processing GNSS data from earthquakes in Chile: Maule M8.8 in 2010 and Iquique M8.2 in 2014

Análise do comportamento do PPP e do TEC ionosférico no pós-processamento de dados GNSS de terremotos ocorridos no Chile: Maule M8.8 em 2010 e Iquique M8.2 em 2014

Lissa Cunha de Almeida[1]; Paulo Sérgio de Oliveira Júnior [2]; Tiago Lima Rodrigues[3]; Maria Vitória Pagno[4]

[1] Federal University of Paraná, PPGCG/Department of Geomatics, Curitiba/PR, Brazil. Email: lcageofisica@gmail.com
ORCID: https://orcid.org/0000-0001-9347-6013

[2] Federal University of Paraná, PPGCG/Department of Geomatics, Curitiba/PR, Brazil. Email: paulo.junior@ufpr.br
ORCID: https://orcid.org/0000-0001-7000-6924

[3] Federal University of Paraná, PPGCG/Department of Geomatics, Curitiba/PR, Brazil. Email: tiagorodrigues@ufpr.br
ORCID: https://orcid.org/0000-0002-3037-9037

[4] Federal University of Paraná, Department of Cartographic Engineering and Surveying, Curitiba/PR, Brazil. Email: mariapagno@ufpr.br
ORCID: https://orcid.org/0009-0004-4986-3074

Abstract: GNSS positioning has been a powerful tool in seismology, enabling to monitoring of crustal movements during seismic events, monitor the influence of the atmospheric gravity waves on the Total Electron Content (TEC), and even quantifying seismic wave, often with significant advantages over land-based seismographs. Therefore, the goal of this study is to contribute to research that employs GNSS in earthquake analysis by identifying seismic signatures in the GNSS positioning and TEC, as well as by analyzing ionospheric disturbances associated with seismic events. Thereby, two case studies were carried out for seismic events in Chile: the Maule earthquake (Mw 8.8) on February 27, 2010, and the Iquique earthquake (Mw 8.2) on April 1, 2014. In this study, PPP solutions and TEC data were analyzed using observations from GNSS stations located near the earthquake epicenters. The details and nature of earthquakes remain challenging through observations of traditional techniques. Therefore, the discussions presented in this article support the application of PPP and also brought some important perspectives for future studies in this area. This is a necessary bias for the implementation of measures aimed at improving the mechanisms responsible for monitoring and preventing high-intensity earthquakes occurrences in vulnerable areas.

Keywords: GNSS positioning; Ionospheric TEC; Earthquake.

Resumo: O Posicionamento GNSS é uma ferramenta poderosa em sismologia capaz de monitorar movimentos crustais em momentos de atividade sísmica, as influências das ondas de gravidade no TEC, e quantificar ondas provenientes de eventos sísmicos de alta intensidade. O objetivo deste trabalho é corroborar com pesquisas que utilizem GNSS em estudos de terremotos, através da busca de assinaturas sísmicas no posicionamento e no TEC. Para tal, dois estudos de caso foram realizados para eventos no Chile, o terremoto em Maule (Mw 8.8), em 27 de fevereiro de 2010, e em Iquique (Mw 8,2), em 1 de abril de 2014. Neste estudo, foram analisadas soluções do PPP e TEC ionosférico, utilizando dados de estações GNSS localizadas nas proximidades do epicentro destes terremotos. Os detalhes e a natureza dos terremotos continuam desafiadores por meio de observações das técnicas tradicionais, sendo assim, as discussões geradas neste artigo suportam a continuidade da aplicação do GNSS em investigações de monitoramento de terremotos e também apresentam perspectivas importantes para estudos futuros na área. Este é um viés necessário para que medidas sejam tomadas no aprimoramento de mecanismos responsáveis pelo monitoramento e prevenção de áreas propensas à ocorrência de terremotos de alta magnitude.

Palavras-chave: Posicionamento GNSS; TEC ionosférico; Terremotos.

Received: 26/02/2025; Accepted: 16/05/2025; Published: 16/06/2025.

1. Introduction

Earthquakes are previously unavoidable geological events, i.e. they are large-scale phenomena that occur suddenly and their frequency is related to the plate tectonics of the region in which they occur (PRESS *et al*., 2006; TEIXEIRA *et al*., 2009). The risks presented by these events to societies living near regions of intense tectonic activity are diverse, involving civil casualties such as landslides, fires and even tsunamis in some cases. Risks like these tend to be mitigated once the region's plate tectonics and the different earthquake monitoring and prevention technologies that can be used are better understood.

The west of the South American continent is a region that suffers from the issue of the vulnerability of its structures, added to the fact that it has densely populated areas in places with moderate to high intensity seismic events. It is therefore important to develop and improve tools that can monitor and help reduce civil risks and casualties. Given these motivations, the aim of this work is to review and evaluate the use of GNSS (Global Navigation Satellite System) data processing and analysis in the context of major earthquakes, specifically events in South America. The main interest is to identify possible seismic signatures in data analysis, such as seismic-ionospheric disturbances and positional variations in GNSS estimations. In this research, these evaluations involve the PPP (Precise Point Positioning) parameters and the total electron content of the ionosphere, known in the scientific community as TEC. Studies carried out in this context have shown promising results with the application of GPS/GNSS positioning in similar cases (NIKOLAIDIS *et al.*, 2001; LIU *et al.*, 2004; HAYAKAWA *et al*., 2011; PEREVALOVA *et al.*, 2014; JIN *et al*., 2015). The discussions in this research support the relationship between seismic waves from large seismic events and their influence on the ionospheric disturbances observed shortly after these events.

2. Methodology

In summary, this research followed the steps shown in the flowchart in figure 1.

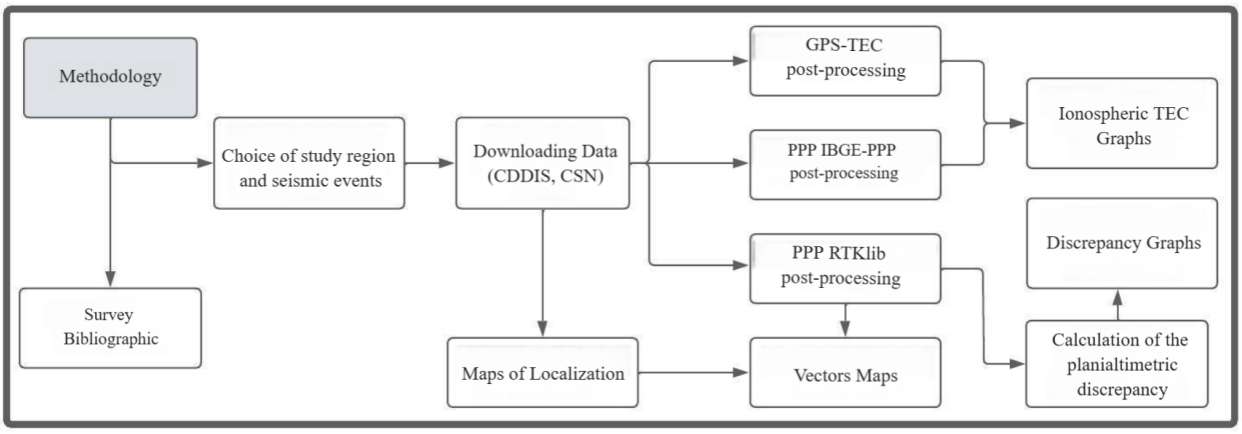

Figure 1 – Methodological sequence employed.
Source: Authors (2025).

The first phase covered the bibliographic survey that was conducted throughout the research and at the same time provided the basis for choosing the study region (Pacific Ring of Fire region) and the case studies to be studied (Maule earthquake in 2010 and Iquique earthquake in 2014). Next, the stations close to the events were mapped and the data from the available stations were extracted from the respective data centers in order to create the location maps and post-process the data; this information is presented in sections 2.1 and 2.2 and their respective subsections. The final phase consisted of creating graphics to display and discuss the results, which can be found in section 3 of this study and its respective subsections.

2.1 Location of seismic events

The Maule earthquake struck in south-central Chile on February 27, 2010 at 03:34 local time (06:34 UTC). The intense tremor, with a moment magnitude of Mw 8.8 and a shallow depth of 22.5 km, lasted around 3 minutes and it's considered to be the sixth largest earthquake ever recorded in history. The Iquique earthquake struck on April 1, 2014 at 20:46 local time (23:46 UTC), with a magnitude of Mw 8.2 and a depth of 25 km, on the west coast of northern Chile, as a result of shallow depth plate riding on the Chilean coast (information obtained from Hayes *et al.*, 2017). Figure 2 shows the location of the epicenter of each of the aforementioned earthquakes (Figure 2.A. representing Maule and Figure 2.B. representing Iquique) and the nearest geodetic stations with available data for each.

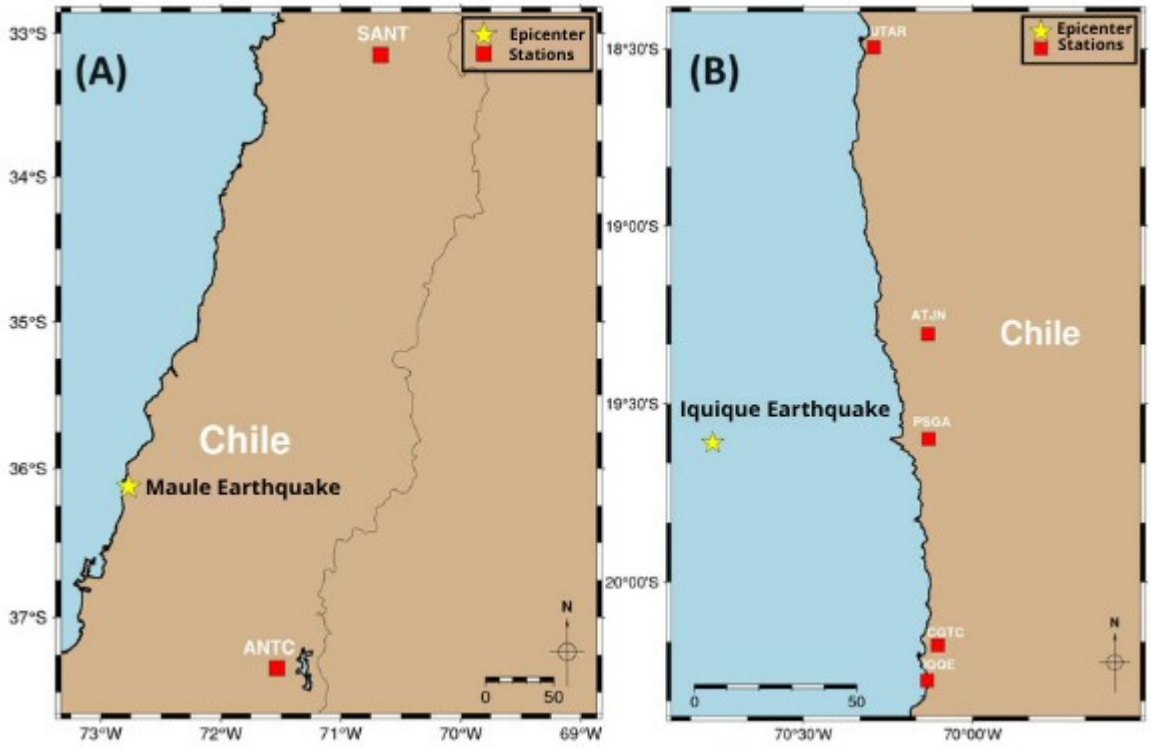

Figure 2 – Map of the epicenters of the Maule (A) and Iquique (B) earthquakes and their respective nearby geodetic stations (IGS/CSN).
Source: Authors (2025).

The characteristics of magnitudes ≥ 6.5 and shallow depth ≤ 40 km were relevant factors in choosing the events for this study. In general, the chances of recording disturbances in the TEC are correlated with the magnitude of the event, which according to Perevalova *et al*. (2014) and their study should respect the Mw ≥ 6.5 threshold. Hayakawa *et al*. (2011) also observed a significant correlation between earthquakes and ionospheric disturbances with events of magnitude greater than 6 and an epicentral shallow depth of less than 40 kilometers. Therefore, the magnitude and epicentral depth of these events were decisive factors for choosing them in this work, maximizing the conditions for their characterization.

Geodetic stations close to the event with available data were mapped and integrated into this study. Table 1 shows the coordinates of each station and their respective distances from the epicenter of the earthquake to which they are related.

Table 1 – Coordinate values and distances of the stations from the epicenter of the earthquake to which they are related.

Station (***IGS/CSN***)	Geographical coordinates		Distance to epicenter (km)
	Lat (°N)	Long (°E)	
MAULE EARTHQUAKE			
ANTC (***IGS***)	- 37.338	- 71.532	180
SANT (***IGS***)	- 33.150	- 70.668	387
IQUIQUE EARTHQUAKE			
UTAR (***CSN***)	- 18.495	- 70.292	127
ATJN (***CSN***)	- 19.304	- 70.131	71
PSGA (***CSN***)	- 19.598	- 70.129	67
CGTC (***CSN***)	- 20.176	- 70.063	102
IQQE (***CSN***)	- 20.275	- 70.134	104

Source: Authors (2025).

The distance of the stations from the epicenter is a parameter that directly influences the monitoring of positional variations associated with earthquakes. The closer the stations are to the epicenter, the greater the disturbance in their position. In the case of this study, the ANTC station is the nearest to the epicenter of the Maule earthquake and the PSGA station is the nearest to the epicenter of the Iquique earthquake.

2.2 Data post-processing

The input data for this work were RINEX (Receiver Independent Exchange Format) files, ephemeris and correction files (clock correction, antenna, tide, differential code and Earth orientation parameters) provided by the IGS (International GNSS Service - https://igs.org/data/) and CSN (National Seismological Center - https://gps.csn.uchile.cl/data/) data centers. Post-processing was carried out using RTKlib software version 2.4.2 (TAKASU, 2020). This software, through the RTKpost module, is able to provide positioning solutions for a range of positioning methods. For this study, the PPP (Precise Point Positioning) method was used, as its positioning solutions can globally achieve accuracy of centimeters to decimeters (KING *et al.*, 2002; GRINTER & ROBERTS, 2011), which is suitable for crustal movement monitoring applications, such as earthquakes. The settings used for post-processing the data are also shown in Table 2.

Table 2 – Processing settings and files used in RTKpost.

PROCESSING SETTINGS	
Positioning mode	PPP static and kinematic
Frequencies / Observable	L1 + L2 / Ionosphere-free
Kalman filter	*Forward*
Constellation	*GNSS*
Ambiguity resolutions	No (*float*)
Tropospheric correction	ZTD estimation (*Zenith Tropospheric Delay*)
Ionospheric correction	Ionosphere-free combination L1 e L2
Elevation mask	10°
Ephemeris	Broadcast + Precise (IGS)
Sampling range	30 seconds
Other corrections	IERS Convention (2010)

Source: Authors (2025).

The Kalman forward filter is applicable to real-time monitoring contexts, and was therefore chosen for the post-processing of the data in this work, providing a perspective of what the monitoring would be like at the time of the event.

Those interested can find more details in the RTKLIB program manual in Takasu (2013), including the respective mathematical formulations applied. It was disregarded the 2nd and 3rd order effects of ionospheric refraction, which represent less than 1% of the total ionospheric effect, as well as the effects of non-tidal oceanic, tidal and non-tidal atmospheric and hydrological loading (SANZ SUBIRANA *et al.*, 2013; PETIT & LUZUM, 2010).

2.2.1 Calculation of planimetric discrepancies

The absolute differences, referred to in this research as discrepancies, were calculated to identify the positional variation of the coordinates at the geodetic stations under study. The discrepancies were calculated using the difference between the calculated coordinates and the reference coordinates, according to Almeida & Dal Poz (2016), in equations 1 and 2. The reference coordinates were the values calculated for February 26, 2010 (in PPP static mode) and the estimated coordinates of the values calculated on the day of the earthquake, the 27th (in PPP kinematic mode). The variations in coordinates in terms of latitude and longitude for the Maule and Iquique earthquakes were analyzed in relation to this reference solution.

$$\Delta\phi_{rad} = |\phi_{calc} - \phi_{calc}|, \quad (1)$$

$$\Delta\lambda_{rad} = |\lambda_{calc} - \lambda_{calc}|, \quad (2)$$

Where,

- $\Delta\phi_{rad}$ and $\Delta\lambda_{rad}$ are the calculated geodesic discrepancies, in radians;
- ϕ_{ref} and λ_{ref} are the geodetic reference coordinates, in radians;
- ϕ_{calc} and λ_{calc} are the estimated geodesic coordinates, in radians.

The following equations were used to convert these values into meters (TORGE, 2001):

$$\Delta\phi_{(m)} = M * \Delta\phi_{rad}, \quad (3)$$

$$\Delta\lambda_{(m)} = N * \Delta\lambda_{rad} * cos\phi, \quad (4)$$

Where M is the radius of curvature of the meridian section and N is the radius of curvature (in meters) of the first vertical section for a given reference ellipsoid, calculated by:

$$M = \frac{a(1-e^2)}{(1-e^2 sen^2\phi)^{\frac{1}{2}}}, \quad (5)$$

$$N = \frac{a}{(1-e^2 sen^2\phi)^{\frac{1}{2}}}. \quad (6)$$

For the GRS80 there are:

- e^2 = 2,0067395 (second eccentricity);
- a = 6.378.137,000 m (GRS80's longest axle shaft);

- b = 6.356.752,314 m (GRS80's smaller axle shaft).

2.2.2 Total Electron Content (TEC) of the Ionosphere

The GPS-TEC software, developed by Gopi Seemala at Boston College, was used to calculate the ionospheric TEC. This program is a useful and simple tool for calculating the ionospheric TEC from GPS data using RINEX observation files (SEEMALA, 2023). The program obtains absolute TEC values, minimizing TEC variability by using the tendencies of the hardware, satellite and receiver, provided by the University of Bern (VALLADARES *et al*., 2009).

TEC analysis was carried out on each visible satellite at three different times: the days before, the days after and the days when the earthquakes actually struck. In order to analyze the influence of geomagnetic activity and ionospheric scintillation on TEC values during the events, the influences of the daily geomagnetic activity index (∑kp) (OIWAKE CHO & KU, 2021) and the ionospheric scintillation index S4 (fourth harmonic) were considered.

The ∑kp estimates the level of geomagnetic activity for the respective day. According to Perevalova *et al.* (2014) when ∑kp ≤ 16 the conditions of the day are considered to be of low geomagnetic activity, while above this (∑kp ranging between 17 and 40) the conditions of the day are considered to be of moderate to strong geomagnetic activity. The S4 index shows the intensity of ionospheric scintillation and is calculated using the formulation on the Scintec Project website (www.inpe.br/scintec/pt/scintil.php). According to Tiwari *et al*. (2011) this index can be classified into categories depending on the intensity of the signal that struck on the day and at the location in question: strong (S4 ≥ 1.0), moderate (0.5 ≤ S4 ≤ 1.0), weak (0 ≤ S4 ≤ 0.5).

3. Results and Discussion

3.1 Maule earthquake

3.1.1 Positional Variation

The results of the RTKlib PPP post-processing for the Maule events are shown in figure 3. It can be seen that at all the stations observed there is a discontinuity in the data due to the earthquake rupture (earthquake time). This discontinuity is seen in the interval between 6 and 7 UTC, with the official recorded time of the Maule earthquake being 6:34 UTC.

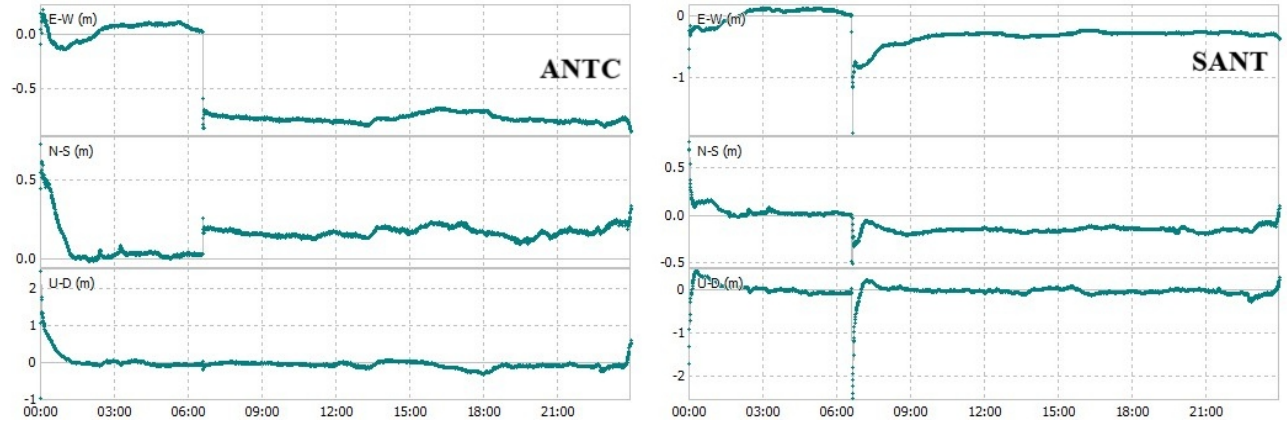

Figure 3 – Post-processing graphs obtained using RTKplot from the ANTC (left) and SANT (right) stations for February 27, 2010.

Source: Authors (2025).

The behavior of the latitudinal and longitudinal variation is similar considering the discontinuity near the time of the earthquake rupture, however the longitudinal component (E-W) shows more considerable variations in the planimetric discrepancy when compared to the latitudinal component (N-S), as also observed by Montecino et al. (2017) within their study. This behavior provides the first indications for inferring the direction of crustal movement, in addition to quantitatively indicating the values for this movement, and may be associated with the direction of subduction of the Nazca plate in relation to the South American plate, which moves eastward (HAYES *et al.*, 2017). Pirti (2024) also presents movement results, from the same stations for the same event, which indicate that at the time of the Maule earthquake there was significant southeast and southwest movement, with greater interference in the horizontal components.

Between the intervals of 6 and 7 UTC it is also possible to observe that the discontinuity that strikes at the moment of rupture for the ANTC station becomes permanent in the subsequent period, while for the SANT station there is a reduction in the difference created by the discontinuity.

To get a closer look at the data, given that the time of convergence of the data occurred briefly, specifically for the Maule earthquake, a cut was made in this time series and the graphs are shown in figure 4. The solutions are shown, displaying the values of the planimetric discrepancies, in meters, for the SANT and ANTC stations.

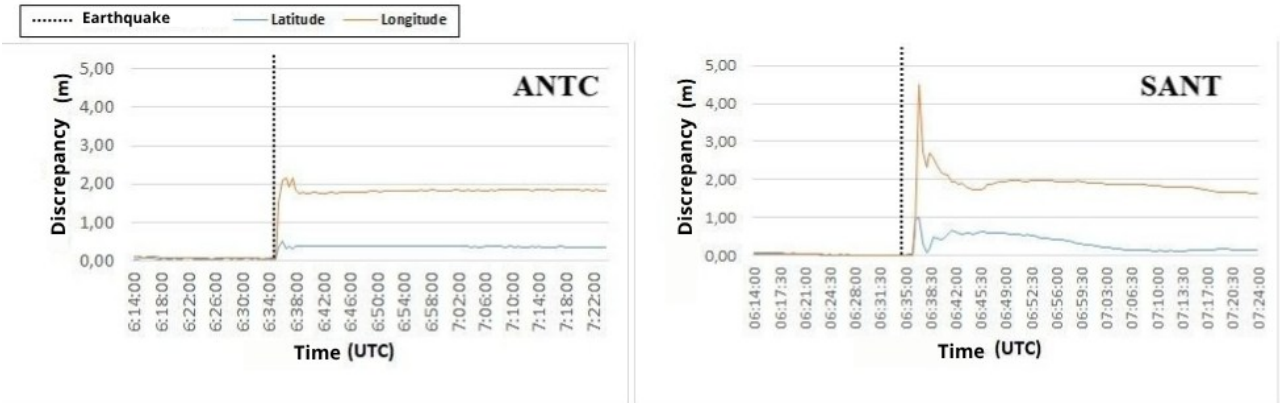

Figure 4 – Time -cut graphs of the planimetric discrepancies obtained using the RTKlib solutions for the ANTC (left) and SANT (right) stations for February 27, 2010.
Source: Authors (2025).

As can be seen in the graphs in figure 4, the solutions for the horizontal components in ANTC showed a variation for the E-W component of approximately 2.2 m, while for the N-S component the variations were between approximately 0.4 m. The average standard deviation for these components was computed with an accuracy of 3-4 cm. The peak occurs approximately 1 minute after the rupture (06:35 UTC). The absolute discrepancy values presented do not necessarily indicate the actual variation suffered by the ANTC station, but rather the difference between the geodetic station's reference position (obtained with the positioning values on the day before the earthquake) and the estimated position (in PPP kinematic on the day of the event) exactly at the time of the earthquake rupture. Therefore, after the event there is a possibility that the station that suffered the greatest variations at the time of the rupture will not maintain this difference in position in the following hours/days.

The discrepancies in the SANT solutions presented are similar to the behavior observed at the ANTC station (jump near the time of the tremor). The greatest variation continues to be in the E-W component and occurs at 06:36 UTC with an amplitude of approximately 4.5 m. Therefore, the graphs shown characterize the moment when the influence of the rupture on positioning occurs, and the delay in this characterization is possibly related to the distance of the station from the epicenter of the earthquake. The ANTC station, which is 180 km from the epicenter, is influenced at least 1 minute earlier than the SANT station, which is 387 km from it.

Another way of visualizing the movement of the event is through displacement vectors. Figure 5 plots the vectors, which show the planimetric directions of movement of the geodetic stations near the epicenter of the quake for February 26, 27 and 28, 2010.

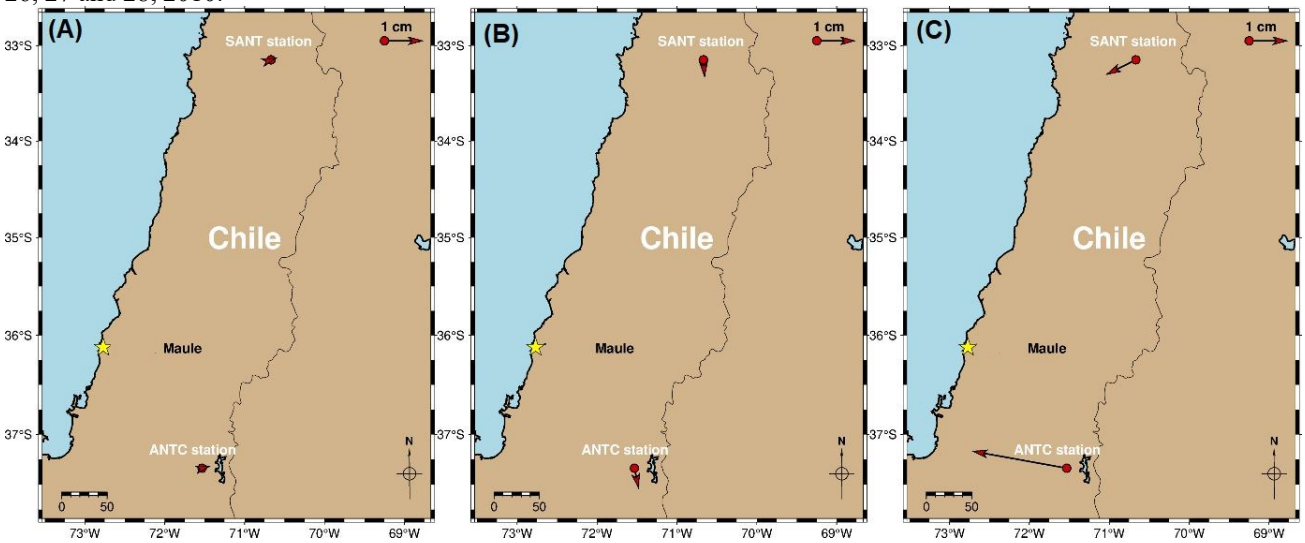

Figure 5 – Displacement direction vectors of geodetic stations near the Maule earthquake for February 26 (A), 27 (B) and 28 (C), 2010.
Source: Authors (2025).

The station closest to the epicenter of the Maule earthquake was ANTC, which showed the greatest permanent positional variation on the day of the earthquake (Figure 5.B.). Its movement is even more apparent through the vectors calculated one day after the earthquake (5.C.). It is expected that the stations closest to the earthquake will show more significant positional variations compared to the other stations, as the mechanical energy produced by such an event is dissipated over the distance between the epicenter and the earthquake.

3.1.2 Ionospheric TEC

At least 6 satellites were “visible” at the time of the Maule earthquake for the ANTC and SANT stations. This section will only present the TEC estimation results for satellites that show possible co-seismic disturbances (PRN20/23) or that have even been analyzed in other works, such as PRN20, which was analyzed by Perevalova et al. (2014) when they analyzed data from the CONZ station, which is currently deactivated and therefore not used in this research.

Looking at the results from the same satellites at the two chosen stations, Figures 6 and 7 present the graphs showing the behavior of the ionospheric TEC curves on the day before (February 26, 2010), after (February 28, 2010), and on the actual day of the earthquake (February 27, 2010). The purpose of comparing these days is also to see how the TEC would behave under “normal” conditions, i.e. conditions in which the earthquake and its repercussions on the ionosphere's total electron content were not present.

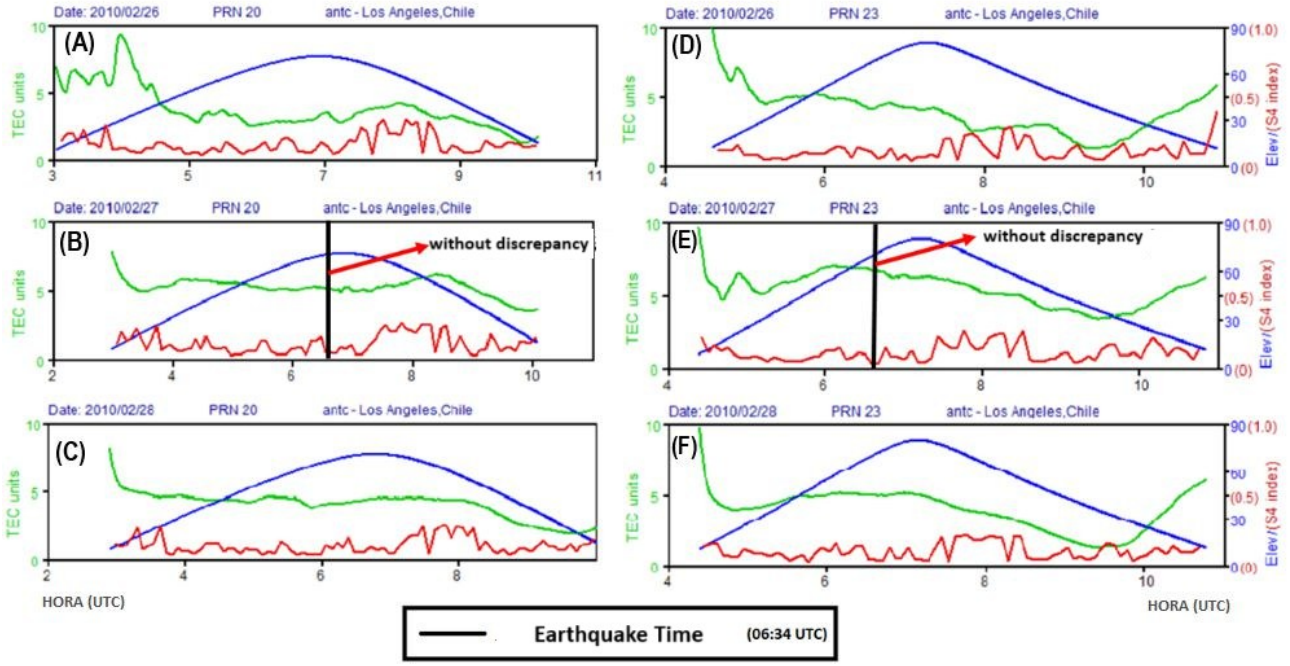

Figure 6 – Behavior of the TEC curve for satellites 20 (A, B, C) and 23 (D, E, F) of the ANTC station on 26, 27 and 28/Feb/2010, time periods close to the earthquake.
Source: Authors (2025).

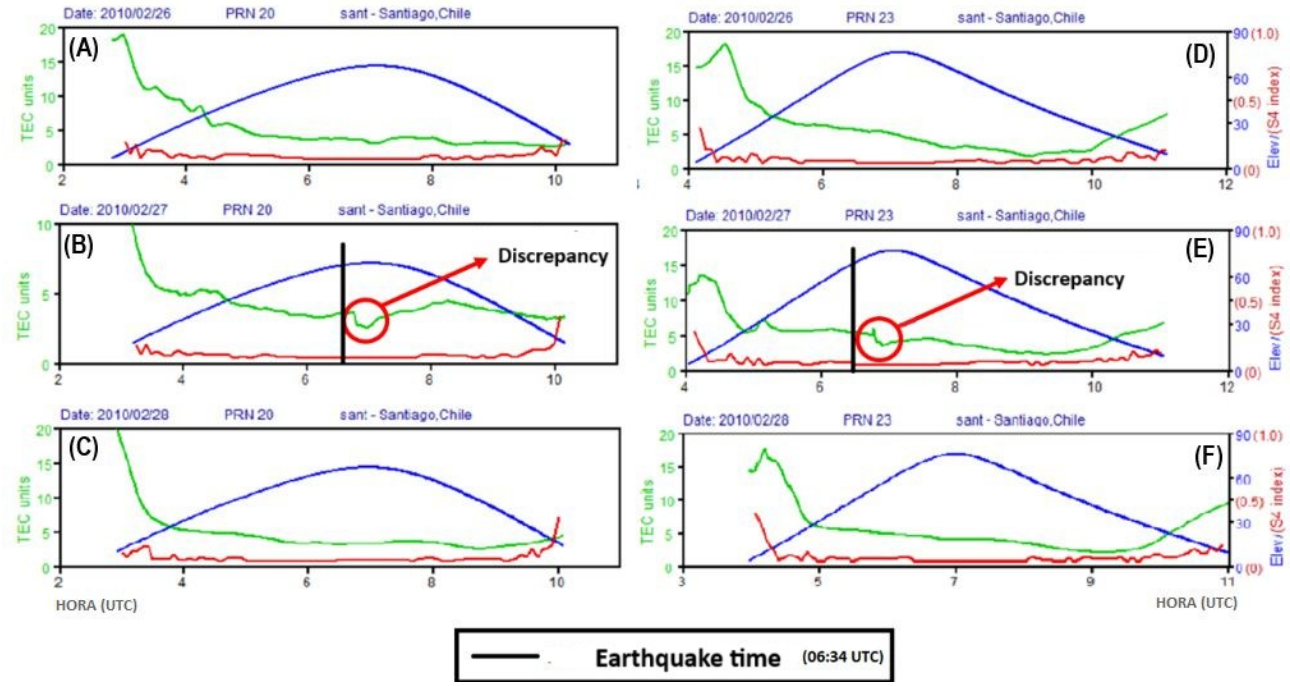

Figure 7 – Behavior of the TEC curve for satellites 20 (A, B, C) and 23 (D, E, F) of the SANT station on 26, 27 and 28/Feb/2010, time periods close to the earthquake.
Source: Authors (2025).

The green line in figures 6 and 7 indicates the variation of the ionospheric TEC in TECU. Diurnal variations in TEC occur due to the incidence of solar radiation, peaking between 12 and 16 hours local time (LT) and a second peak occurs in low latitude regions, between 21 and 22 hours (LT). The values of the S4 index (red curve), which maps the intensity of ionospheric scintillation, when lower than 0.7 allow us to state that there was weak ionospheric activity during the period observed (SOUZA *et al*., 2015). Using the definition of Perevalova *et al*. (2014), which determined the intensity thresholds of the ∑kp index, it was considered that the Maule earthquake occurred under calm geomagnetic conditions, which can be due to the period of low solar activity, with ∑kp = 2 on this day.

Figure 6 shows the behavior of the ionospheric TEC observed at the ANTC station in relation to satellites 20 and 23. There is no evidence of any anomalous variation that interrupts the continuity of the TEC curve close to the time of the earthquake. Figure 7 shows the behavior of the ionospheric TEC for the same satellites, but in relation to the SANT station. In this case, the continuity in the behavior of the TEC is interrupted and it is possible to observe small variations, of approximately 1 TECU for satellite 20 and 2 TECU for satellite 23, in the TEC estimates close to the time of the earthquake.

Jin *et al*. (2015) in their investigation of ionospheric seismology analyzed two seismic events: Wechuan Mw 8.0 in 2008 and Tohoku Mw 9.0 in 2011. For the Wechuan earthquake, smaller disturbance amplitudes were detected and its maximum value was 0.5 TECU, with a short duration of the disturbance. For the Tohoku earthquake, significant seismic-ionospheric disturbances are found above 2 TECU. In this way, the magnitudes of the discontinuities presented in the TEC permeate values that are acceptable in scientific circles and may indicate the influence of the seismic waves from this earthquake on the ionospheric TEC.

3.2 Iquique earthquake

3.2.1 Positional Variation

The results of the RTKlib PPP post-processing for the Iquique events are shown in figure 8. As with the Maule tremor, there is a discontinuity in the data due to the earthquake rupture. This discontinuity occurs between 23:30 and 24 UTC, with the official time of the Iquique earthquake being 23:46 UTC. Figure 8 shows the planimetric discrepancies for the 5 permanent GNSS/CSN stations closest to the earthquake (ATJN, CGTC, IQQE, PSGA and UTAR).

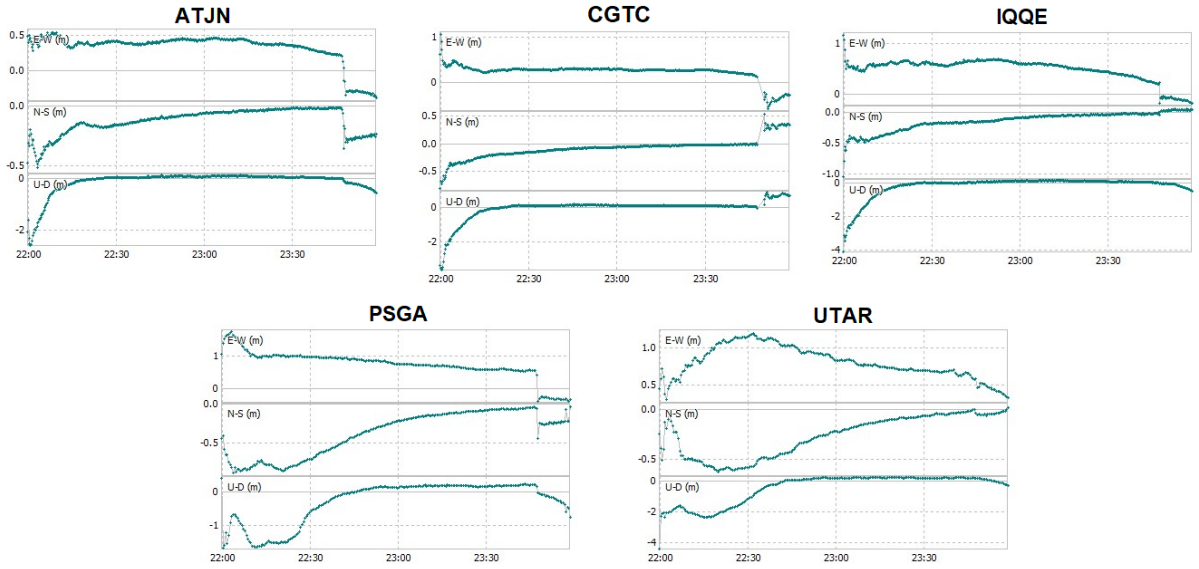

Figure 8 – Planimetric discrepancy for the 5 CSN stations (ATJN, CGTC, IQQE, PSGA and UTAR) near the Iquique tremor. Arranged over a 2-hour interval that encompasses the time of the tremor (23:46 UTC).
Source: Authors (2025).

The time section shown in the graphs above shows an interval of 2 hours of data (between 22-24 UTC). This type of cut-off aims to look specifically at the time surrounding the seismic event. The positional variation of the coordinates at the stations shown close to the time of the earthquake can be seen. It can also be seen that the closest stations, such as PSGA and ATJN, suffered greater variations in their positioning, especially in the horizontal components, with a maximum discrepancy value of approximately 0.7 meters. The average standard deviation for these components was computed with an accuracy of 10-15 cm.

As with the Maule tremor, the displacement vectors of the IQQE, CGTC, PSGA, ATJN and UTAR stations were analyzed with respect to the positions preceding the earthquake. Figure 9 presents a visualization of the results, which show the planimetric directions of movement of the geodetic stations near the epicentre of this earthquake.

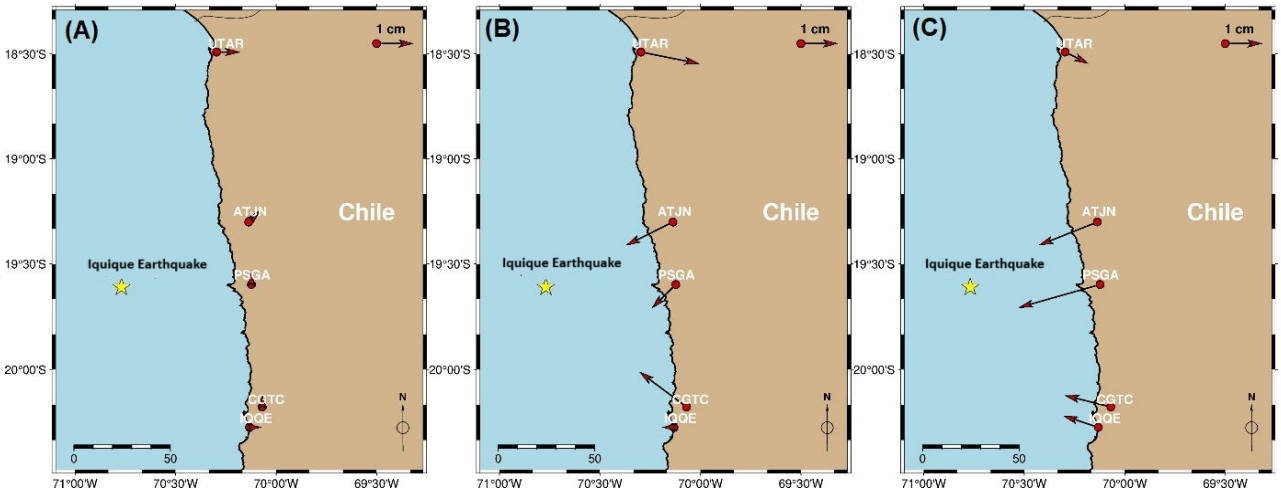

Figure 9 – Displacement direction vectors of geodetic stations near the Iquique earthquake for (A) March 31, (B) April 1 and (C) April 2, 2014.
Source: Authors (2025).

It can be observed that the distance between the stations in the Iquique earthquake is much less than the distance between the stations in the Maule earthquake (Figure 5). The stations closest to each other do not differ so much in their direction of displacement, such as the ATJN and PSGA stations and the CGTC and IQQE stations. However, the more distant stations, such as UTAR, do not follow the same directional pattern for the Iquique earthquake. These changes in the direction of movement of the stations are to be expected, given that regions where plates meet, especially over large areas, can have points with different directions of movement related to the behavior of smaller faults.

3.2.2 Ionospheric TEC

For the stations close to the earthquake, at least 8 "visible" satellites were observed. Figure 10 shows the behavior of the TEC for satellites PRN19 and PRN32, tracked by the IQQE station. Figure 11 presents the results for satellites PRN19 and PRN23, tracked by the UTAR station. Figure 12 presents the results for satellites PRN19 and PRN32, tracked by the PSGA station.

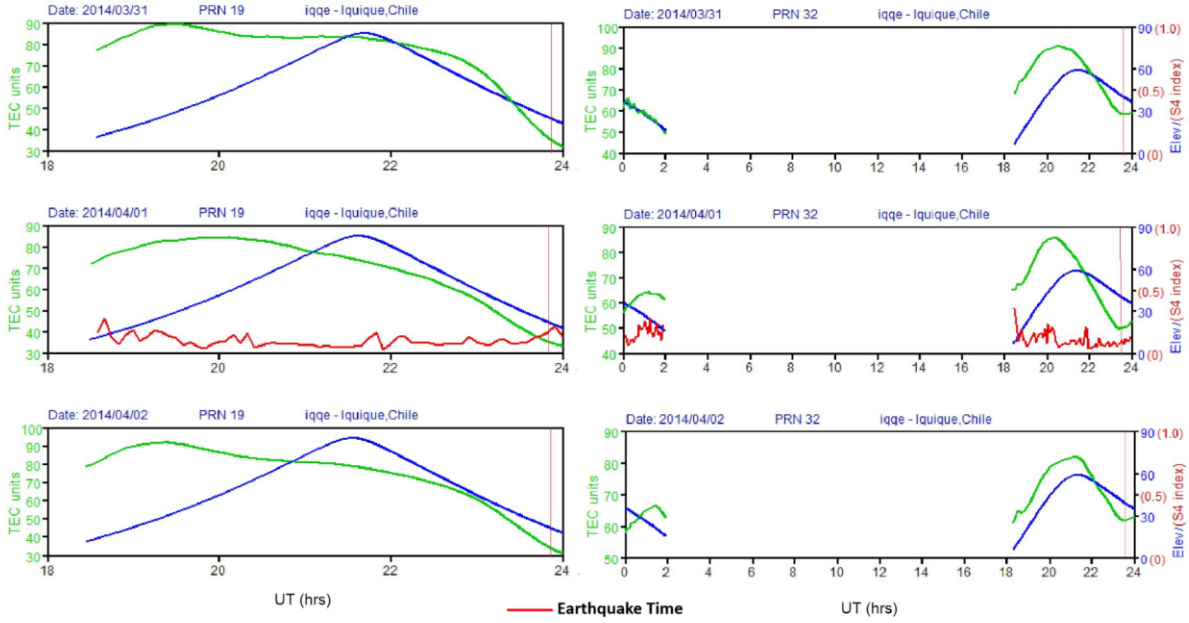

Figure 10 – Behavior of the TEC curve for satellite 19 and 32 of the IQQE station on March 31 and April 2, 2014. Source: Authors (2025).

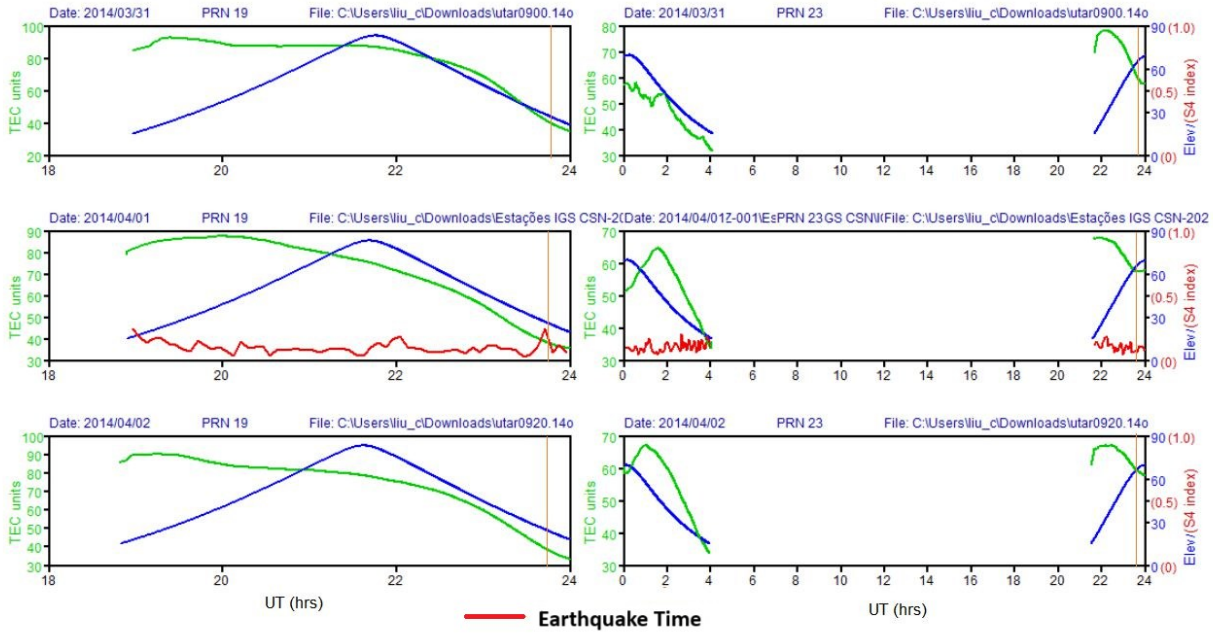

Figure 11 – Behavior of the TEC curve for satellites 19 (left) and 23 (right) of the UTAR station on March 31st and April 2nd, 2014.
Source: Authors (2025).

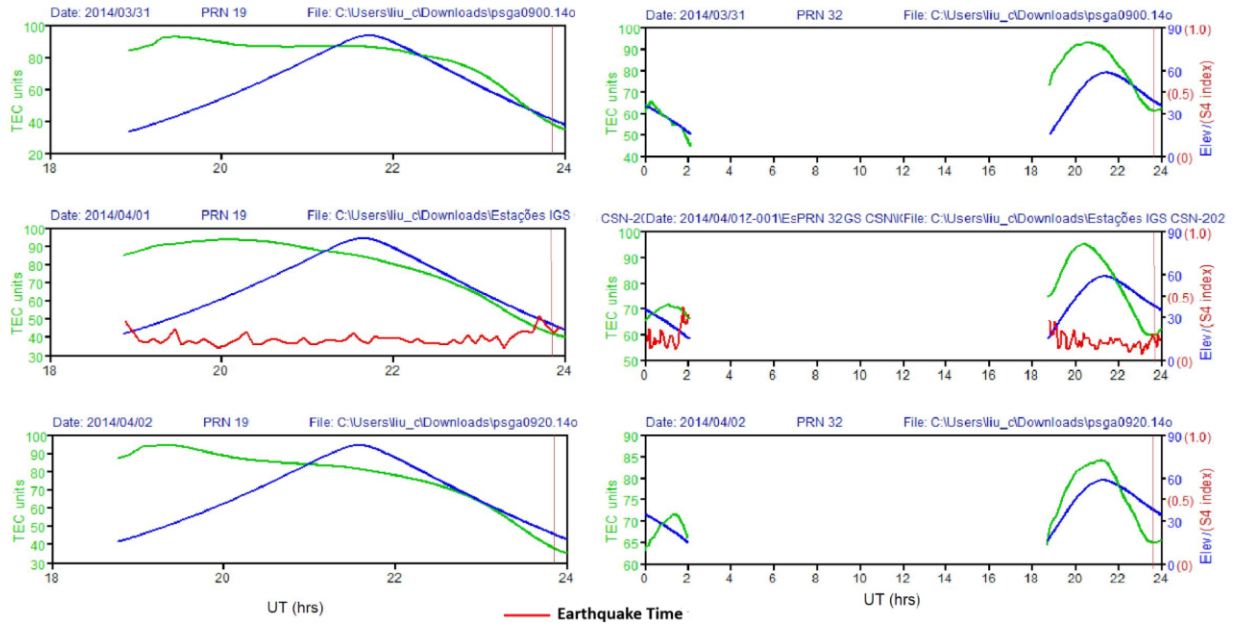

Figure 12 – Behavior of the TEC curve for satellite 19 and 32 at the PSGA station on March 31st and April 2nd, 2014.
Source: Authors (2025).

Despite the lack of information on a large part of the sample from satellite 32 (PRN 32), what was taken into account when choosing this satellite was the fact that it contained a sufficient data interval up to the time of the earthquake, of at least 2 hours before the tremor.

Based on the results of the ionospheric TEC values estimated at the stations closest to the epicenter of the Iquique earthquake, it was not possible to identify evidently visible co-seismic variations in the ionospheric parameter. It is possible that the geometry of the satellites and/or the arrangement of the stations in relation to the epicenter of the earthquake, or even the angle of capture of these satellites, made it difficult to characterize the disturbance in the case of the Iquique earthquake. These are limitations present in this type of approach, especially in regions where there is no dense network of stations.

4. Final considerations

The objectives proposed in this study were partially achieved, since some applications had limitations, which were noticed during the analysis of the data, such as the limitations mentioned about GPS-TEC. On the other hand, this research reinforced the applicability of earthquake monitoring using GNSS positioning, specifically the PPP kinematic method. With this approach, it was possible to compute discrepancies in the horizontal components with centimeter accuracy. By analyzing the planimetric variations, it was possible to get a quantitative idea of the positional variations in seismic events, as shown by the estimated discrepancy values. It was also possible to relate the effect of the distance between the geodetic stations and the earthquake epicenter, i.e. the closer the stations were to the epicenter, the more significant the positional variation observed was. Finally, it was possible to observe the displacement vectors on three different days, thereby observing the direction of movement of the geodetic stations.

The TEC results presented did not show a pattern in relation to the earthquakes studied, given that only one station in the Maule earthquake (SANT Station) showed a variation possibly associated with the event. It was found that TEC is a sensitive parameter, considering that external conditions such as geomagnetic activity, ionospheric scintillation and even the geometry of the satellites and the layout of the stations can influence the results. The most recent studies showing promising results in earthquake characterization through TEC analysis generally rely on a dense geodetic network (i.e. approx. 3000 stations in Japan), which clearly helps to better characterize this parameter. However, the region studied still faces a certain shortage of stations, given the real need to increase the number of geodetic stations in regions with high tectonic activity, such as Chile. The importance of developing methods that can make up for this shortfall is reinforced, making it possible to monitor earthquakes even in unsuitable conditions in order to guarantee the safety of the population living in such regions.

In summary, this study supports the integration of GNSS positioning methods and ionosphere analysis (TEC, ionosonde) for monitoring seismic events, given the direct relationship between these approaches in earthquake contexts. Furthermore, it is recommended for future work that studies be carried out on other earthquakes in South America, with characteristics of intensity and epicentral depth that are similar to the events studied here, with a focus on the preventive detection of co-seismic signatures, since it was not possible to cover this aspect in this research. Another aspect that deserves attention is the pursuit of integrating geodetic data with in situ data, i.e. using records from seismographs in the region to be studied, in order to cooperate in a better understanding of the components of the rupture initiation processes and their relationship with atmospheric phenomena. Regarding the effects on the ionosphere, it is essential to explore other available resources, such as studies that allow imaging of the ionosphere or techniques for representing the ionosphere with greater resolution, such as ionospheric maps (2D) and even so-called ionospheric tomography (3D).

References

ALMEIDA, M. S.; DAL POZ, W. R. *Posicionamento por ponto preciso e posicionamento relativo com GNSS: Qual é o método mais acurado atualmente?* Boletim de Ciências Geodésicas, v. 22, n. 1, p. 175–195, 2016.

CDDIS. *CDDIS* |. Available on: <https://cddis.gsfc.nasa.gov/>. Accessed at: 2 out. 2021.

GRINTER, T.; ROBERTS, C. *Precise point positioning: where are we now*. International global navigation satellite systems society IGNSS symposium. Anais...Citeseer, 2011.

HAYAKAWA, M. et al. *Atmospheric gravity waves as a possible candidate for seismo-ionospheric perturbations.* Journal of Atmospheric Electricity, v. 31, n. 2, p. 129–140, 2011.

HAYES, G. P. et al. *Tectonic summaries of magnitude 7 and greater earthquakes from 2000 to 2015.* [s.l.] US Geological Survey, 2017.

JIN, S.; OCCHIPINTI, G.; JIN, R. *GNSS ionospheric seismology: Recent observation evidences and characteristics*. Earth-Science Reviews, v. 147, p. 54–64, 2015.

KING, M.; EDWARDS, S.; CLARKE, P. *Precise point positioning: Breaking the monopoly of relative GPS processing*. Engineering Surveying Showcase, v. 10, n. 2002, p. 33–34, 2002.

LIU, J. Y. et al. *Pre-earthquake ionospheric anomalies registered by continuous GPS TEC measurements.* 2004.

MONTECINO, H. D. et al. *Effects on Chilean Vertical Reference Frame due to the Maule Earthquake co-seismic and post-seismic effects*. Journal of Geodynamics, v. 112, p. 22–30, 2017.

NIKOLAIDIS, R. M. et al. *Seismic wave observations with the Global Positioning System*. Journal of Geophysical Research: Solid Earth, v. 106, n. B10, p. 21897–21916, 2001.

OIWAKE CHO, K.; KU, S. *WDC for Geomagnetism*, Kyoto. Disponível em: <http://wdc.kugi.kyoto-u.ac.jp/>. Acesso em: 12 abr. 2021.

PEREVALOVA, N. P. et al. *Threshold magnitude for ionospheric TEC response to earthquakes.* Journal of Atmospheric and Solar-Terrestrial Physics, v. 108, p. 77–90, 2014.

PETIT, G.; LUZUM, B. *IERS conventions (2010)*. Tech. Rep. DTIC Document, v. 36, p. 180, 1 jan. 2010.

PIRTI, A. *Investigation and prediction of the 2010 Maule, Chile earthquake by using GNSS on 25, 26 and 27 February 2010.* Journal of South American Earth Sciences, v. 133, p. 104702, 2024.

PRESS, F. et al. *PARA ENTENDER A TERRA.* 4. ed. [s.l.] Bookman, 2006.

SANZ SUBIRANA, J.; JUAN ZORNOZA, J. M.; HERNÁNDEZ-PAJARES, M. *GNSS Data Processing*, Volume I: Fundamentals and Algorithms. ESA Communications, ESTEC, Noordwijk, Netherlands, p. 145–161, 2013.

SEEMALA, G. K. Chapter 4 - *Estimation of ionospheric total electron content (TEC) from GNSS observations.* Em: KUMAR SINGH, A.; TIWARI, S. (Eds.). Atmospheric Remote Sensing. Earth Observation. [s.l.] Elsevier, 2023. p. 63–84.

SOUZA, J. S.; ALVES, D. B. M.; VANI, B. C. *Estudo do comportamento da Cintilação Ionosférica em diferentes regiões brasileiras e seu impacto no posicionamento GNSS*. Revista Brasileira de Cartografia, v. 67, n. 1, p. 97–109, 2015.

TAKASU, T. RTKLIB ver. 2.4. 2 *Manual. RTKLIB: An Open Source Program Package for GNSS Positioning*, p. 29–49, 2013.

TAKASU, T. *RTKLIB*. Tokyo, Japan, 29 dez. 2020. Available on: <https://rtklib.com/>

TEIXEIRA, W. et al. *Decifrando a Terra*. 2009.

TIWARI, R. et al. *WBMod assisted PLL GPS software receiver for mitigating scintillation effect in high latitude region.* 2011 XXXth URSI General Assembly and Scientific Symposium. Anais...IEEE, 2011.

TORGE, W. *Geodesy*, 3a. edition. [s.l.] Walter de Gruyter GmbH & Co, 2001.

VALLADARES, C. E. et al. *Simultaneous observation of traveling ionospheric disturbances in the Northern and Southern Hemispheres*. Ann. Geophys, v. 27, n. 4, p. 1501–1508, 2009.